Peptides in motion

Poloni, Claudia

Chapter 5

Light and heat control over secondary structure and amyloid fiber formation in an overcrowded-alkene-modified Trp zipper

The external photocontrol over peptide folding, by the incorporation of molecular photoswitches into their structure, provides a powerful tool to study biological processes. However, it is limited so far to switches that exhibit only a small geometrical change upon photoisomerisation and that show thermal instability of the photoisomer. Here we describe the use of an overcrowded alkene photoswitch to control a model β-hairpin peptide. This photoresponsive unit undergoes a large conformational change and has two thermally stable isomers which has major influence on the secondary structure and the aggregation of the peptide, permitting the phototriggered formation of amyloid-like fibrils.

This chapter is based on:
C. Poloni, M. C. A. Stuart, P. van der Meulen W. Szymanski, B. L. Feringa, *Chem. Sci.* 2015, **6**, 7311-7318.

5.1 Introduction

Amyloidogenic peptides are the precursors of cytotoxic fibers, for example in Alzheimer and Parkinson diseases.[1,2,3] Research on these medicinally relevant peptides aims at understanding the process and the mechanism behind the fibril formation. β-Hairpin peptides are the basic units of the amyloidogenic fibrils and the proper design of their sequence can lead to the development of inhibitors for amyloidogenesis.[4]

Recently, considerable effort has been devoted to the synthesis of responsive β-hairpin, which can be controlled with external stimuli, such as pH,[5] temperature[6] and ionic strength,[7] among others. Of special interest are systems that use light to modulate peptide folding in order to control biological function.[8] As opposed to the above-mentioned stimuli, light can be delivered with very high spatial and temporal precision and control over the intensity and wavelength of irradiation. The creation of light- responsive peptide hybrids relies on covalent introduction of molecular photoswitches.[8,9] Several photoresponsive β-hairpins were synthesized by incorporating either azobenzene,[10,11,12,13] stilbene,[14] or hemithioindigo[15] photochromic units into the putative turn-region of the β-hairpin structure. These powerful tools have already shown their potential in delivering insights into the mechanism and kinetics of β-hairpin formation and, through that, information on the process behind the formation of cytotoxic fibrils involved in different diseases.[11, 16, 17] Photoswitchable β-hairpins are also considered for their ability to form hydrogels: they can be useful in tissue engineering, drug delivery and biosensing.[10] Simple β-hairpins, bearing an azobenzene unit, have been used to modulate viscoelasticity of a peptide hydrogel. [10] However, the small number and insufficient structural diversity of molecular photoswitches that have been evaluated for their use in controlling peptide conformation limits the scope of potential photoregulated systems. Of particular importance is the fact that switches used so far induce only rather small geometrical changes upon photoisomerisation. Furthermore, in all cases only two photoisomeric states can be addressed, one of which is usually thermally unstable.

Here we report, for the first time, the application of an overcrowded-alkene-based switch[18] for the control of a β-hairpin peptide structure (Figure 1b). This overcrowded alkene switch has two stable stereoisomers, *trans* and *cis* form, which strongly differ in shape and helicity. The conversion between these two states occurs *via* an intermediate, a metastable stereoisomer (unstable-*cis*) with a half-life in the order of days (Figure 1b). Irradiation of the *trans* isomer leads to *trans-cis* isomerisation of the central olefinic bond and formation of the unstable *cis* isomer. Thermal relaxation of this form leads to helicity inversion and stable *cis* isomer is obtained. Irradiation of the stable *cis* isomer provides a short-lived unstable *trans* isomer, which, on the scale of

seconds at room temperature, undergoes transformation into the stable *trans* form, thereby completing a four-stage switching cycle of the overcrowded alkene switch.

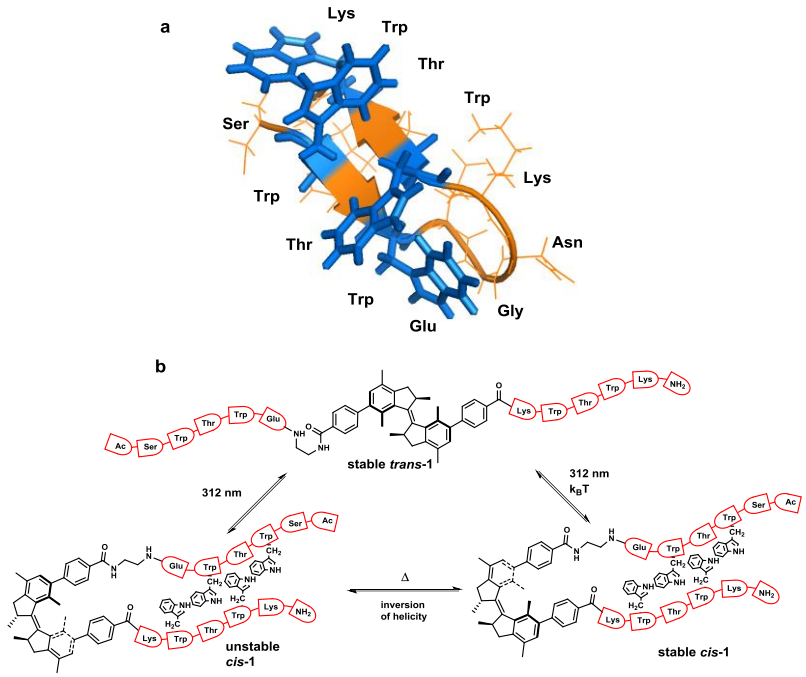

Figure 1: Trpzip modified with overcrowded alkene. a) Trpzip reported by Cochran et al.[22] b) Rotary cycle for β-hairpin bearing overcrowded alkene. Picture created from PDB 1LE0 (ref 22).

We expected that this photoresponsive molecule, upon introduction into a peptide backbone, would provide more information on the mechanism and dynamics of the formation of secondary structure, as compared to conventional photoswitches; for example, the metastable stereoisomer could offer the possibility to reveal the presence of intermediates of this process in a spatially and temporally controlled manner. Of importance is also the presence of more than one thermally stable forms that can be accessed with light, which could permit to follow the processes behind the peptide folding without being affected by the thermal reisomerisation, as is in the case of azobenzenes and hemithioindigos. Moreover, the photoisomerization between the stable states imposes a different geometrical change compared to azobenzenes or other switches used so far. The overcrowded alkene switch was already successfully used for tuning the enantioselectivity of reactions,[18,19] photocontrolling magnetic interactions[20] and ion binding by light.[21] Here, we show that an overcrowded alkene switch can be used to control peptide conformation and aggregation.

The β-hairpin sequence (Figure 1a), used in our design, is called trpzip and it was introduced by Cochran, Starovasnik and co-workers.[22] The trpzips[22] are stable β-hairpins and they fold in a monomeric form without requiring metal binding. They are

stabilized by cross-strand pairs of indole rings. The turn region can vary in composition: the pair NG favors a turn I' while GN or ^{D}PN favor turn II' (Figure 1a).[22] In our approach, the overcrowded alkene switch was inserted in the turn region and we analysed the effect of photoisomerization on the secondary structure. We envisioned that the *trans* photoisomer of the overcrowded alkene switch wouldn't mimic the turn and therefore it wouldn't form any defined structures, while the stable and unstable *cis* stereoisomer, by bringing the two strands in close proximity, would promote β-hairpin structure formation. This would permit photo-triggered formation of secondary structure of a β-hairpin peptide. Notably, trpzip peptide was already modified by Moroder[23] with an azobenzene switch at the same position, which allows to compare the effects of the overcrowded alkene and the azobenzene switches.

5.2 Results and Discussion

Synthesis. For the convenient and generally-applicable preparation of peptides with an overcrowded alkene introduced into the peptide backbone, we have described in chapter 4 a switch-bearing building block **2** (Figure 2; in Chapter 4, compound 7) that can be applied in standard Fmoc-based solid phase peptide synthesis (SPPS). The synthesis of compound **2** has been described in Chapter 4. The β-hairpin-switch hybrid **1** (Figure 1b) was synthesised by a standard protocol for Fmoc SPPS, using building block **2** (Figure 2a). As reported in the previous chapter, the use of a highly acid-sensitive Sieber amide resin, together with acid-sensitive protecting groups for the side-chains, like Trt and O-2-Ph*i*Pr, permitted the use of a cleavage cocktail with <50% of TFA and led to the isolation of the desired bis-peptide-overcrowded alkene product. The product *trans*-**1** was purified by semi-preparative HPLC and lyophilized. MALDI-TOF confirmed the product and the purity was found by HPLC to be 96% (Figure 2).

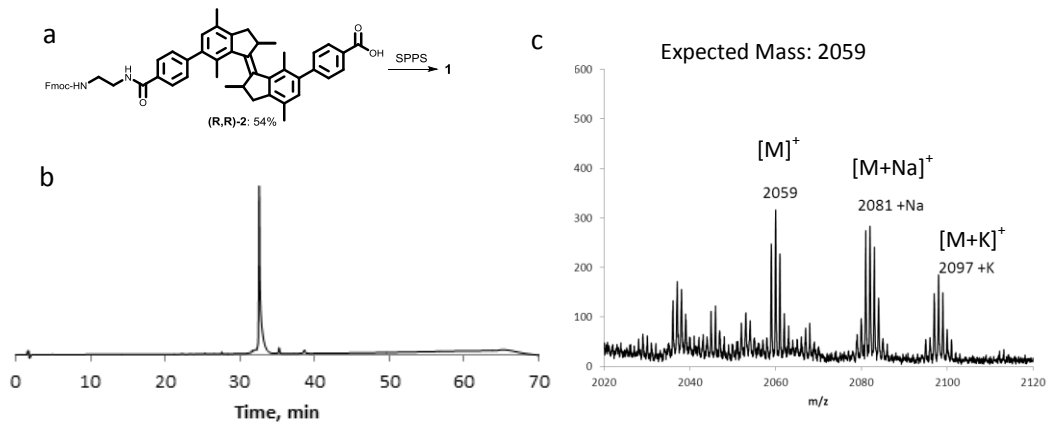

Figure 2: Synthesis and characterization of compound **1**. a) Synthesis of **1** from precursor **2**. b) HPLC traces (detection wavelength: 220 nm) for purified product **1**. c) MALDI-TOF spectrum for product **1**.

Switching cycle of overcrowded alkene-bis-peptide. UV-vis and NMR spectroscopies are generally used to study the switching cycle of overcrowded alkenes.[18,20] The isomerisation around the double bond is induced by light and heat and it is accompanied by inversion of helicity (Figure 1b). Irradiation of *trans*-**1** isomer at λ = 312 nm leads to the unstable *cis*-**1** isomer, which is characterised by the appearance of a band at 350 nm in the UV-vis spectrum. Unstable *cis* isomer converts to stable *cis* form in a thermal isomerization process, which is accompanied by the disappearance of the 350 nm absorption band. If irradiation at λ = 312 nm is applied to the stable *cis* isomer at low temperature, the unstable *trans* stereoisomer is presumably formed, which quickly undergoes relaxation to the stable *trans* from.[18,19,21,24]

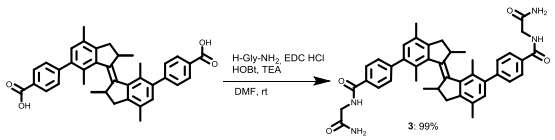

Scheme 1: Synthesis of compound **3**.

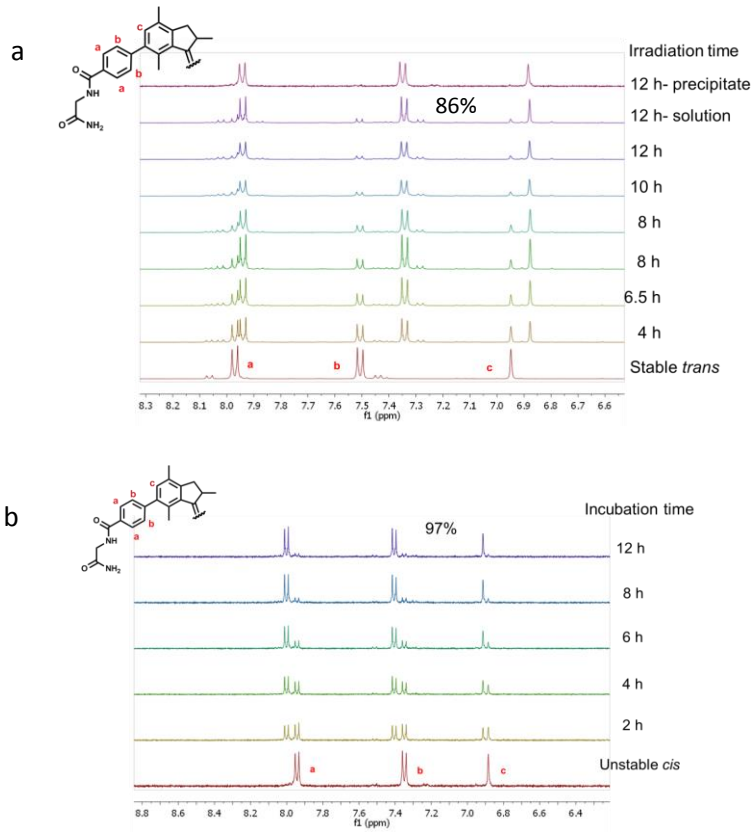

Figure 3: a) Irradiation at λ = 312 nm of *trans*-**3** (5 mg in 500 uL CD_3OD) followed in time by ^1H NMR (aromatic region). b) Thermal isomerization at 40 ˚C of unstable *cis*-**3** (15 mM) followed in time by ^1H NMR (aromatic region).

To study the influence that the modification of an overcrowded alkene with a β-hairpin peptide has on its switching cycle, we synthesized and analysed reference compound **3** (Scheme 1). This molecule is a similar overcrowded alkene switch functionalized with two glycinamides *via* amide bond, representing the simplest bis-peptide-bearing overcrowded alkene switch. The PSS of compound **3** was studied by NMR (Figure 3) and it was determined to be *trans*:unstable *cis* 14:86 in methanol (Figure 3a). The following process, the isomerization from unstable to stable *cis* resulted to be quantitative after 12h irradiation (Figure 3b).

We compared the kinetics of the switching cycle of compounds **1** and **3** and analysed the thermodynamic parameters, both the entropic and enthalpic terms (Figure 4), reasoning that differences in the enthalpic term would imply interactions between the two strands in compound **1**. On the other hand, the possible difference in the entropic term could be attributed to the increased length of the peptidic side chains in **1**, compared to **3**, since the rotation in **1** would require more pronounced reorganization of solvent molecules.[25]

The switching cycle of **1** was studied in methanol, using HPLC as an additional analytical method, besides CD, UV-vis spectroscopy and NMR. The irradiation of *trans*-**1** at λ = 312 nm for 2-15 min leads to unstable *cis*-**1**: the photostationary state (PSS) was determined by HPLC to be 93:7 unstable *cis*:*trans* (Figure 4a). Subsequently, the thermal isomerisation, from unstable *cis*-**1** to stable *cis*-**1**, was achieved by warming the sample up at 40-50 °C for 4-6 h. While HPLC analysis shows that there is no significant difference in polarity between unstable *cis*-**1** and stable *cis*-**1** (Figure 4b, c), this transformation is apparent from the change in the UV-vis spectrum (Figure 4d) and NMR spectrum (Figure 6b, see below for discussion). The decrease in absorbance at λ = 350 nm, corresponding to the conversion of unstable *cis*-**1** to the stable form, was followed in time at different temperatures and the thermodynamic parameters were calculated using the Eyring equation (Figure 4f). The established Gibbs free energy of activation ($\Delta^{\ddagger}G°$) is 104 KJ mol^{-1}, the enthalpy of activation ($\Delta^{\ddagger}H°$) is 90 KJ mol^{-1} and the entropy ($\Delta^{\ddagger}S°$) at rt is -46 J mol^{-1} K^{-1}. The half-life of unstable *cis*-**1** is 4.1 d at rt. A similar study was performed on model compound **3**, giving the $\Delta^{\ddagger}G°$ of 102 KJ mol^{-1} and the half-life of 2.2 d at rt (Figure 4f). The difference in $\Delta^{\ddagger}G°$ for the thermal helix inversion between compounds **1** and **3** is mainly due to the entropic term (Figure 4f,g). Therefore we attribute the difference in kinetics not to the formation of secondary structure but to the mobility of the two arms connected to the switch, either due to aggregation or to the length of the these two arms as reported for an overcrowded alkene modified with different arms acting as a molecular stirrer.[25] In fact, the isomerisation is affected by the length of the rigid substituents in viscous solvents and the differences in kinetics are dominated by entropy effects.[25]

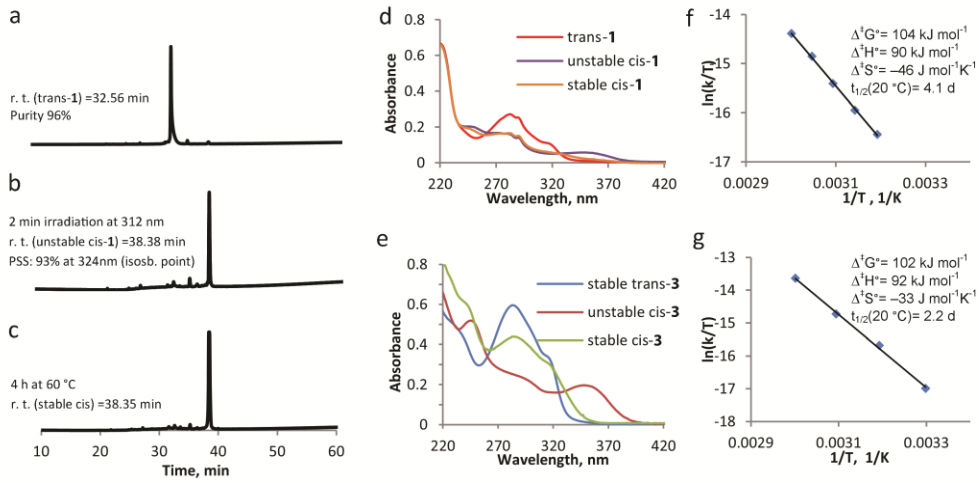

Figure 4: Switching cycle for modified β-hairpin **1** and model compound **3** followed by UV-vis spectroscopy and HPLC. a) HPLC trace for *trans*-**1**. b) HPLC trace after 2 min irradiation at λ = 312 nm to form unstable *cis*-**1**. c) HPLC trace after 4 h at 60 °C to form stable *cis*-**1**. d) UV-vis spectra of *trans*-**1**, unstable *cis*-**1** and stable *cis*-**1**. e) UV-vis spectra of *trans*-**3**, unstable *cis*-**3** and stable *cis*-**3**. (f) Eyring plots obtained by following the decrease in absorbance at 350 nm at different temperatures, with the associated activation parameters for the transition unstable *cis*-stable *cis*, for compound **1**. (g) Eyring plots obtained by following the decrease in absorbance at 350 nm at different temperatures, with the associated activation parameters for the transition unstable *cis*-stable *cis*, for compound **3**.

Circular Dichroism. Circular dichroism (CD) spectroscopy provides additional information about the structure of the peptide; π-π stacking of the indole side chains of the tryptophan moieties has been reported as an indication of β-hairpin formation in trpzip peptides.[13,22] The CD spectrum for the β-hairpin shows an exciton coupling at λ = ~220 nm.[26] When indole groups of the tryptophans interact with each other, typically an increase of molar ellipticity of this band is observed.[22] Temperature influences the stacking of tryptophans and, therefore, it is possible to determine the temperature of denaturation of β-hairpin, following the decrease of the molar elipticity of the band at λ = 220 nm as a function of temperature.[22]

The CD spectrum of compound **1** has two components: the CD signals due to the overcrowded alkene chromophore and those resulting from the tryptophan indole groups. To estimate the first of these components, a simple switch compound **4** (Figure 5) was analysed (Figure 5a). The switch contributes strongly to the CD spectrum in the range of 200-400 nm: the CD spectrum of compound **4** in the *trans* form shows two positive signals at 243 nm and at 285 nm; the unstable *cis* form shows one positive signal at 253 nm and one negative signal at 295 nm, while the stable *cis* has a negative signal at 249 nm and a positive one at 286 nm, comparable to results

reported previously for other overcrowded alkenes.[18] The helical inversion during the isomerization of unstable *cis* to stable *cis* is evident from the change in sign for the bands at ~250 nm and at ~290 nm (Figure 5a).

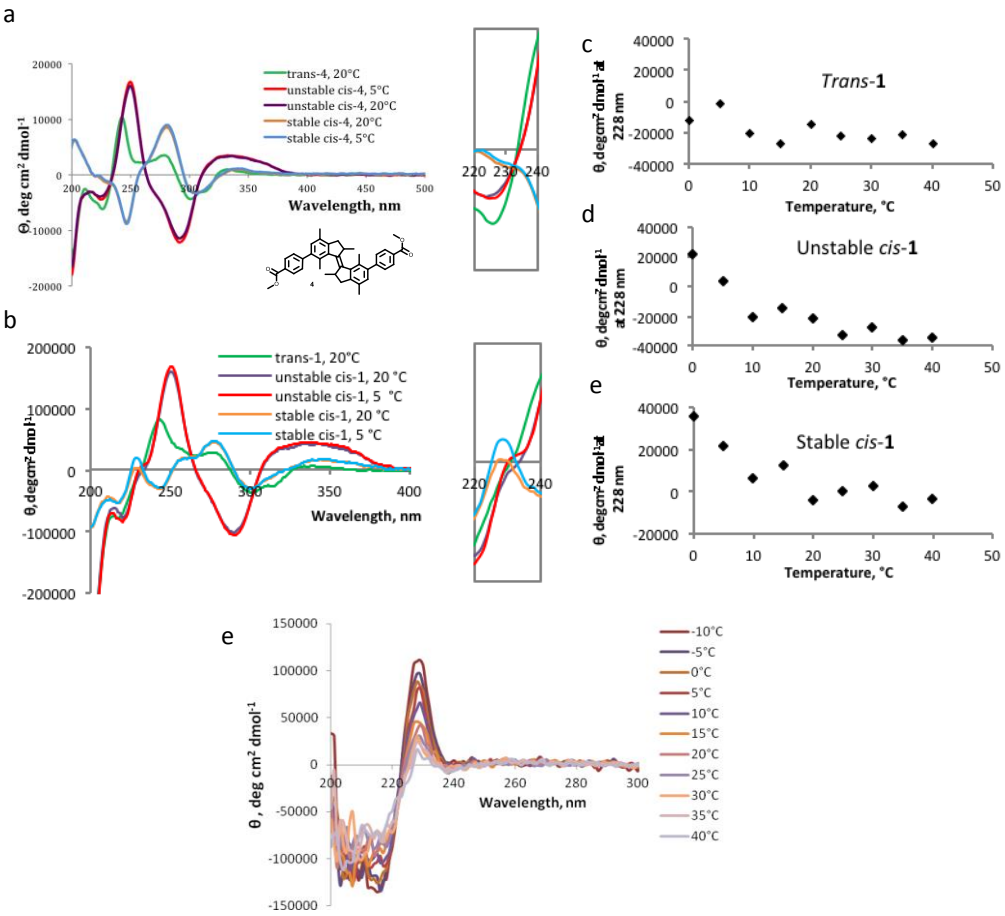

Figure 5: CD spectra for modified β-hairpin **1** and compound **4**. a) CD spectra of *trans*-**4** at 20 °C, unstable *cis*-**4** at 20 °C and 5 °C, stable *cis*-**4** at 20 °C and 5 °C (24 μM in methanol). Inset: zoom in on the corresponding band at 230 nm. b) CD spectra of *trans*-**1** at 20 °C , unstable *cis*-**1** at 20 °C and 5 °C, stable *cis*-**1** at 20 °C and 5 °C (24 μM in methanol). Inset: zoom in on the corresponding band at 230 nm. c) Molar elipticity (θ) at 228 nm for *trans*-**1** at different temperatures. d) Molar elipticity (θ) at 228 nm for unstable *cis*-**1** at different temperatures. e) Molar elipticity (θ) at 228 nm for stable *cis*-**1** at different temperatures. f) CD spectra of natural Trp-zipper β-hairpin at different temperatures.

As compared to the results obtained for compound **4**, the CD spectra of compound **1** show an additional band at 228 nm, which is characteristic for the tryptophan

moiety (Figure 5b).[22] For unstable *cis*-**1** and stable *cis*-**1**, the molar ellipticity of the band at 228 nm increases when the temperature is decreased, while for the *trans* form it remains largely unchanged (Figure 5c, d, e). This temperature-dependence indicates that, especially at low temperature, unstable *cis*-**1** and stable *cis*-**1** can form the β-hairpin structure, while *trans*-**1** does not. It is not possible to precisely quantify the content of β-hairpin, because the CD absorption band at 228 nm has a strong contribution of the switch unit, especially for unstable *cis*-**1**. As a control, the native trp-zipper (Figure 1a) was synthesized by SPPS and analysed by CD spectroscopy. For stable *cis*-**1**, the content in secondary structure at 0 °C can be estimated to be ~50% compared to the natural β-hairpin (Figure 5f).

NMR Study. With an indication on the formation of β-hairpin from the CD measurements, we further studied the nature of this folded structure by NMR analysis of the peptide hybrid **1** in methanol-d_3: a solvent, which was also used for the study of β-hairpin peptide modified with azobenzene.[13] ^{1}H-NMR, COSY, TOCSY and NOESY spectra were recorded, a set that provides the possibility to assign the proton signals in proteins or peptides using Wüthrich's method.[27] The measurements were performed for the three different isomers of peptide-switch hybrid **1**. *Trans*-**1** gives very sharp signals in the spectra (See 1D- and 2D-NMR studies of compound **1**, Experimental section), indicating the presence of monomeric species. All the protons in the backbone and in the side-chains were identified, apart for the indole signals of the tryptophans. NOE signals between amino acids in the two strands of the overcrowded alkene were not found (Figure 6a). The irradiation at λ = 312 nm promotes the formation of unstable *cis*-**1** and subsequent warming up at 50 °C for 4h leads to the formation of the stable *cis*-**1**. These two processes were monitored by following the shift of the signals of the two methyl groups in the allylic position of the overcrowded alkene (Figure 7a, b). In the *trans* form, the chemical shift values corresponding to these protons are 1.08 and 1.13 ppm (Figure 7a); in the unstable *cis* form, one of these protons is visible at 1.52 ppm (Figure 7a). Although the PSS ratio is >9:1, it was not possible to identify clearly the signals of the peptidic region in the *cis* forms. Unfortunately the durations of the NMR experiments are in the same range as the thermal stability of the unstable *cis* isomers, therefore structural information can be obtained only for stable *cis* form. For the stable *cis* form, the protons mentioned above have a chemical shift of 1.13 ppm (Figure 7b). Based on the number of signals for every amino acid (for example Lys-6, Figure 7c) in the stable *cis* form, it seems that two or more species coexist. Such multiplication of NMR signals has been observed before, e.g. in the case of peptide GNNQQNY, and was attributed to the formation of aggregates of different architecture.[28] To exclude any degradation of the *cis* forms that would lead to new species visible in NMR spectra, the stable *cis*-**1** was purified by

semi-prep HPLC and again analysed by NMR. The NMR study for stable *cis*-**1** was conducted at rt and 5 °C (See 2D-NMR studies on compound **1**, Experimental section). At rt, the NMR spectra were sharp and well-resolved, and few weak cross peaks between the two strands were observed that became more intense upon decreasing the temperature (Figure 6b). At 5 °C, the peaks became broader and two or more coexistent structures were formed (for example shown for the Lys-6 signals, Figure 7c). The decreased temperature, probably, provokes aggregation; it was not possible to reverse the process by increasing the temperature.

In summary, *trans*-**1** does not seem to adopt any secondary structure and exists in a monomeric state. Unstable and stable *cis*-**1** form aggregates and the decrease in temperature promotes this process. There is more than one pattern of signals for some amino acids (Lys-6, Thr-3, Thr-8) and this behaviour is attributed to the coexistence of more than one type of aggregate.[28]

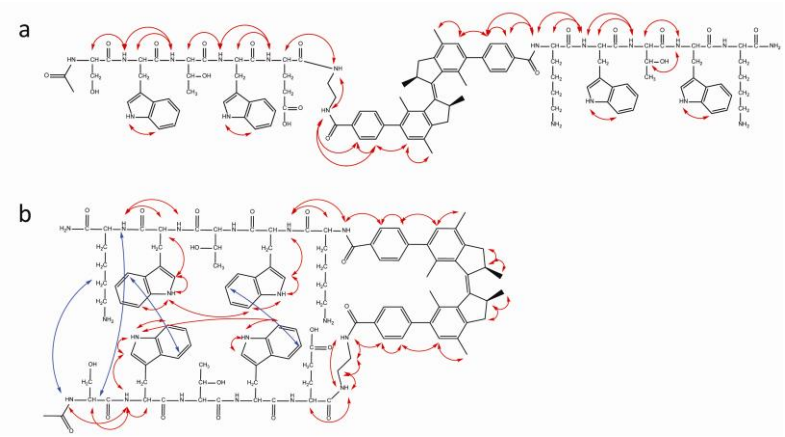

Figure 6: Cross peaks scheme obtained from NOESY NMR spectra. a) NOE signals for *trans*-**1** (2.9 mM in methanol-d_3) at rt. b) NOE signals for *cis*-**1** (2.9 mM in methanol-d_3) at 5 ˚C. Red lines indicate intra-strand cross peaks and blue lines indicate inter-strand cross peaks. See experimental section for the spectra.

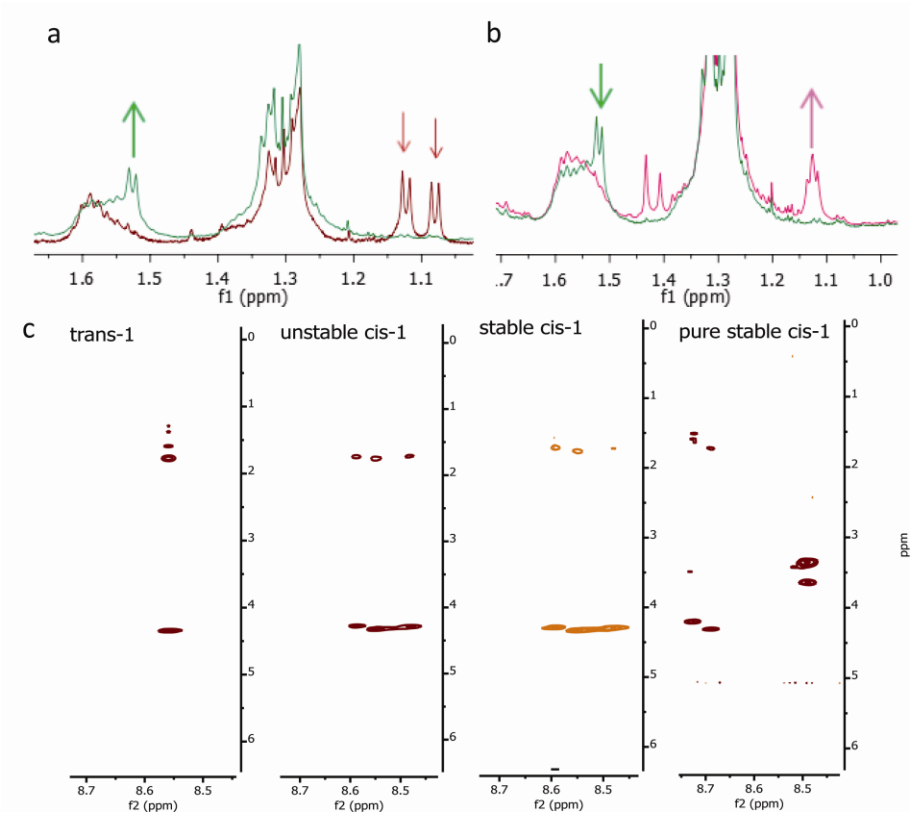

Figure 7: Switching cycle for the modified β-hairpin **1** followed by NMR spectroscopy. a) Characteristic region for the CH_3 signals before irradiation (*trans*-**1**; red line) and after irradiation (unstable *cis*-**1**; green line) at 312 nm. b) Characteristic region for the CH_3 signals before (unstable *cis*-**1**; green line) and after warming up at 50 °C for 4 h (stable *cis*-**1**; pink line). c) TOCSY signals (8.5 - 8.7 ppm) for Lys-6 for *trans*-**1**, unstable *cis*-**1** and stable *cis*-**1** at rt and the purified stable *cis*-**1** at 5 °C. (For full spectra, see experimental section).

TEM and cryo-TEM. To identify the structure formed upon aggregation of compound **1**, we used transmission electron microscopy (TEM) and cryo-TEM. These techniques have been successfully used to study the morphology and the mechanism of assembly of amyloids.[29,30,31,32] Hybrid β-hairpin **1** was studied both in water and in methanol.

In methanol, *trans*-**1** forms vesicles (Figure 8a), while the stable *cis*-**1** shows the formation of different aggregates, vesicles and fibers (Figure 8b,c). The fibers are similar to those formed by amyloidogenic peptides (Figure 8f).[17,31,32,33] This aggregation behaviour is a further indication that the synthesized hybrid peptide in stable *cis* form adopts a β-hairpin structure. The presence of different aggregates, vesicles and fibers, can explain the coexistence of patterns of signal for the same amino acid in the NMR studies. Probably the hybrid peptide goes through a phase transition phenomena: the

fibers are formed from vesicles as recently reported, for example, for the peptide Ac-KLVFFAE-NH_2.[29] In our system it is possible to visualize this transition state, indicated with an arrow in Figure 8b and detailed in Figure 8d, consistent with native amyloid Aβ(16-22) (Figure 8e).[29]

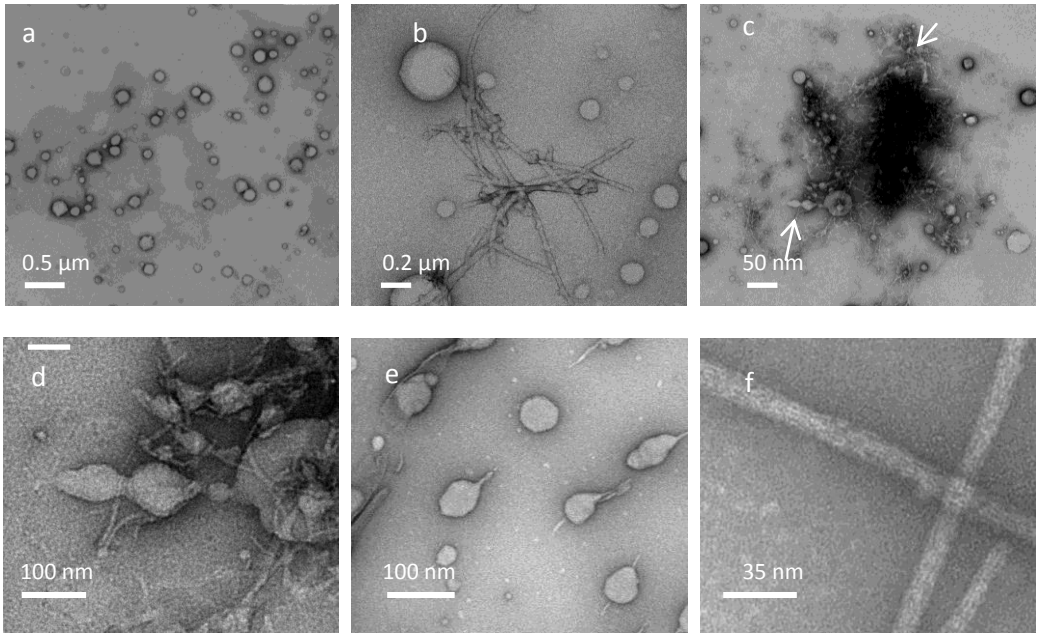

Figure 8: TEM images for the different stereoisomers of **1**. a) TEM image for *trans*-**1** in methanol. b, c) TEM image for stable *cis*-**1**. Arrows indicate the transition state from vesicles to fibers. d) Zoom of TEM image b. e,f) Native amyloid β, Aβ(16-22) in buffer. Figures e,f adapted from Ref. 29. Copyright 2012 American Chemical Society.

In water, *trans*-**1** shows strong aggregation behaviour, as shown by cryo-TEM (Figure 9a) and sheet-like structures are formed. The irradiation-promoted isomerisation to unstable *cis*-**1** (Figure 9b) and subsequent heating, to form stable *cis*-**1**, disrupt this sheet-like structure, and almost no aggregation is observed by cryo-TEM (Figure 9c). The aggregation of *trans*-**1** can be explained by comparison to a system where β-hairpin was modified with *trans*-azobenzene.[10,12] The system in the *trans* form is flexible enough to be able to adopt an extended conformation. This facilitates interfibrillar cross-linking.[10] Although it is clear that in both cases the hybrids form interconnected structures, the aggregates look different in cryo-TEM images compared to the ones found by Nilsson and coworkers:[10] the overcrowded alkene photoswitch induces sheet-like structures in water (Figure 9a) and not fibril-like structures as seen with azobenzene peptide.[10] The sheet-like structures are probably formed due to the fact that the two strands of different molecules interact, but we

believe that also the highly hydrophobic core of the overcrowded alkene promotes aggregation in a different manner than azobenzene (Figure 9).

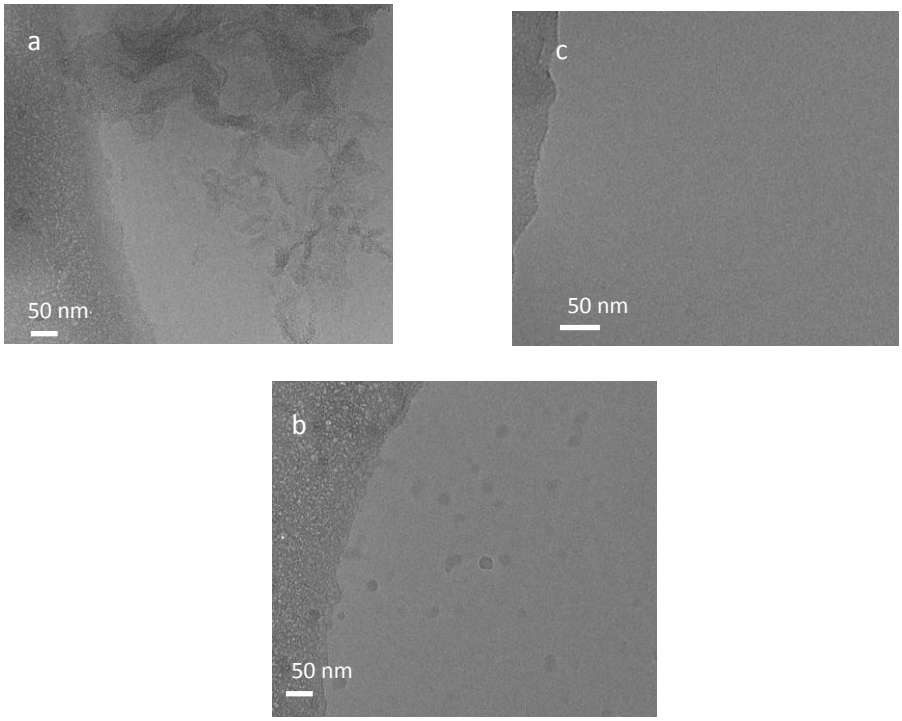

Figure 9: Cryo-TEM images for the different stereoisomers of **1**. a) Cryo-TEM image for *trans*-**1** (1 mg/mL) in water. b) Cryo-TEM image for unstable *cis*-**1** (1 mg/mL) in water. c) Cryo-TEM image for stable *cis*-**1** (1 mg/mL) in water.

To further study if peptide **1** in the *cis* configuration forms aggregates in water, fluorescence measurements were performed using Nile Red,[34] which is a very sensitive probe for domains that differ in polarity. If the system is homogeneous, the probe is constantly in the same environment; with one species present, the change in excitation wavelength does not cause a change in emission wavelength. If the probe is exposed to environments of distinct polarity, e.g. due to the existence of hydrophobic aggregates in the solution, the protonation state of the probe is different which leads to the co-existence of species with different fluorescence properties. Therefore, by changing the wavelength of excitation, multiple species will be addressed, which will lead to the change in emission wavelength. For compound **1** in all the stereoisomers, the maximum wavelength of emission changes with the excitation wavelength (Figure 10). Therefore we conclude that two *cis* forms are indeed forming apolar aggregates in water.

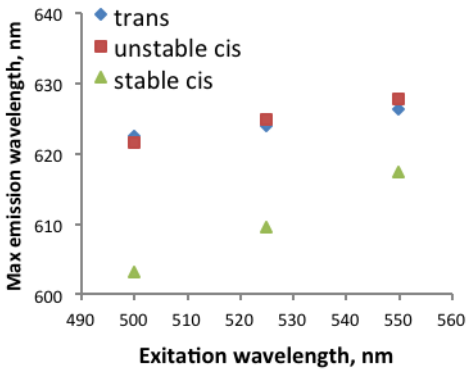

Figure 10: Nile red experiment. Plot of the excitation wavelengths (500 nm, 525 nm, 550 nm) versus the emission wavelengths maxima for *trans*-**1** (1 mg/mL in water), unstable *cis*-**1** (1 mg/mL in water) and stable *cis*-**1** (1 mg/mL in water) after addition of 2 µL Nile Red (0.25 mM in ethanol).

5.3 Conclusions

An overcrowded alkene molecular switch that can be used as a building block for solid phase peptide synthesis was designed, synthesized and used as a responsive unit in a β-hairpin-forming peptide. It demonstrated to be an excellent photoresponsive element to control biomolecule structure and organisation: even when inserted in the peptide, the light- and heat-induced transformations from *trans*-**1** to unstable *cis*-**1** and to stable *cis*-**1** are very selective processes characterized by high conversions. Notably, the unstable *cis* stereoisomer offers a different chiral environment than the stable *cis* form and, due to its metastability, it could be used as a tool for the study of dynamics of secondary structure formation. The photochemistry, isomerisation cycle, secondary structure and aggregation of **1** were studied in detail in methanol. CD and NMR showed that *trans*-**1** does not form any ordered structures, while the unstable and stable *cis*-**1** show the characteristic behaviour of peptides that adopt a β-hairpin structure. At higher concentration, the *trans* stereoisomer forms vesicles but, in the *cis* forms, co-existing structures are observed in NMR. The TEM measurements confirmed that different aggregates, fibers and vesicles, are present simultaneously. Transition phase aggregates could also be observed. Importantly, *cis*-**1** in methanol forms structures associated with amyloidogenic peptides.[29]

In water, hybrid peptide **1** also forms aggregates, as observed by cryo-TEM. In particular, *trans*-**1** shows sheet-like structures that can be disrupted by irradiation, while the *cis* stereoisomers seem to form aggregates, although simple precipitation cannot be excluded.

Interestingly, the aggregates formed by the *trans* stereoisomer are very different from the ones obtained by modifying the same β-hairpin with an azobenzene.[10] In general, the spatial arrangement that the three stereoisomers of the overcrowded alkene switch provoke are different than the one given by azobenzene switches.[10,13,16] The introduction of this overcrowded alkene switch, therefore, opens new possibilities not only to study biological processes, but also to create new bio-compatible and bio-inspired tunable materials, taking advantage of the bistability of the overcrowded alkene switch.

5.4 Acknowledgments

We thank Prof. R. M. Scheek and Prof. W. R. Browne (Faculty of Mathematics and Natural Sciences, University of Groningen) for discussions.

5.5 Experimental Section

5.5.1 Synthesis

All chemicals for the synthesis were obtained from commercial sources and used as received unless stated otherwise. Solvents were reagent grade. Thin-layer chromatography (TLC) was performed using commercial Kieselgel 60, F254 silica gel plates, and components were visualized with $KMnO_4$ or phosphomolybdic acid reagent. Flash chromatography was performed on silica gel (Silicycle Siliaflash P60, 40-63 m, 230-400 mesh). Drying of solutions was performed with $MgSO_4$ and solvents were removed with a rotary evaporator. Chemical shifts for NMR measurements were determined relative to the residual solvent peaks ($CHCl_3$, δ = 7.26 ppm for hydrogen atoms, δ = 77.0 for carbon atoms). The following abbreviations are used to indicate signal multiplicity: s, singlet; d, doublet; t, triplet; q, quartet; m, multiplet; br s, broad signal. 2D NMR spectra were recorded in CD_3OH at 20 °C and 5 °C on a Agilent 600. The 2D TOCSY spectra were recorded with a spin-lock period of 70 ms. 2D NOESY spectra were recorded with mixing times of 400 to 600 ms. HRMS (ESI) spectra were obtained on a Thermo scientific LTQ Orbitrap XL. MALDI spectra were obtained on a MALDI/TOFTOF 4800 by AB Sciex; the analysis was done in positive mode using the matrix alpha-cyano-hydroxycinnamic acid. Solid phase peptide synthesizer CEM Liberty, with CEM Discover microwaves was used for solid phase peptide synthesis. Optical rotations were measured on a Schmidt + Haensch polarimeter (Polartronic MH8) with a 10 cm cell (c given in g/100 mL) at 20 °C. Melting points were recorded using a Buchi melting point B-545 apparatus. UV/Vis absorption spectra were recorded on an Agilent 8453 UV-Visible Spectrophotometer using Uvasol-grade solvents. CD spectra were recorded on a CD spectrophotometer JASCO J815. Irradiation experiments were performed with a spectroline ENB-280C/FE UV lamp (312 nm). RP-HPLC was carried out with Shimadzu equipment using a linear gradient of 1.54% of eluent A per min at a flow rate of 0.5mLmin^{-1}. The eluents A and B are 0.1 % TFA acetonitrile and 0.1 % $_{aq}$TFA, respectively. For analytical RP-HPLC, a XTerra C18 3.0x150mm column (Waters) was used and for semi-preparative RP-HPLC, a XTerra Prep C18 7.8x150mm column (Waters) was used.

Synthesis of *trans*-3

To a solution of racemic *trans*-dicarboxylic acid (compound **6**, Chapter 4) (73 mg, 0.13 mmol, 1 eq) in 1 mL DMF: CH_2Cl_2 (1:1), EDC·HCl (49 mg, 0.26 mmol, 2.0 eq) and HOBt (4.7 mg, 2.0 eq) were added. After 30 min, glycinamide hydrochloride (8.5 mg, 2.0 eq) and TEA (35 uL, 2.0 eq) were added. After 24 h, 50 mL AcOEt was added and the organic phase was washed with 1N $_{aq.}$HCl solution (2 x 50 mL), brine (1 x 50 mL), $_{sat.aq.}NaHCO_3$ solution (2 x 50 mL) and again brine (1 x 50 mL). The organic layer was dried and the solvent was evaporated. The product was isolated as a white powder (45 mg , 0.067 mmol, yield = 56%). m.p. 210 °C (dec.); ^{1}H NMR (400 MHz, DMSO-d_6) δ, 8.22 (2H, 2 N**H**), 7.97 (d, *J* = 8.3 Hz, 4H, arom), 7.55 (d, *J* = 8.3 Hz, 4H, arom), 7.39 (s, 2H, N**H**$_2$), 7.04 (s, 2H, N**H**$_2$), 6.97 (s, 2H, arom), 3.84 (d, 4H, C**H**$_2$ Gly), 3.12 – 2.97 (m, 2H, C**H**CH$_3$), 2.55 (m, 2H, C**H**$_2$CHCH$_3$), 2.26 (m, 2H, C**H**$_2$CHCH$_3$), 2.26 (s, 6H, C**H$_3$** ar), 2.23 (s, 6H, C**H$_3$** ar), 1.08 (d, *J* = 6.4 Hz, 6H, CHC**H$_3$**). ^{13}C NMR (400 MHz, DMSO-d_6) δ 171.1, 166.2, 144.8, 141.6,

141.6, 139.9, 132.4, 131.2, 129.5, 129.2, 127.8, 127.3, 42.5, 41.8, 38.5, 28.9, 21.0, 19.1, 17.9. Expected ESI Mass ($C_{42}H_{45}N_4O_4$): 669.3435. Found: 669.3434.

Synthesis of 1: Ac-Ser-Trp-Thr-Trp-Glu-switch-Lys-Trp-Thr-Trp-Lys-NH_2

The switch-peptide hybrid **1** was synthesized on a 0.009 mmol scale by standard protocol of Fmoc chemistry SPPS. Sieber resin was used (0,69 mmol/g). Fmoc-Trp-OH, Fmoc-Lys(Trt)-OH, Fmoc-Thr(Trt)-OH, Fmoc-Glu(O-2-PhiPr)-OH, Fmoc-Ser(Trt)-OH were used. The coupling steps were performed with 5 eq Fmoc-protected amino acid, 5 eq HBTU and 10 eq DIPEA (2 x 45 min). The Fmoc-deprotection step was performed with 20% piperidine in DMF (1 x 30 min). The acetylation step was performed with 10 eq Ac_2O, 0.1 eq HOBt and 10 eq DIPEA. Cleavage from the resin was performed at 0 °C for 1 h with TFA:DCM (1:3) with 2.5 $_{vol}$% 2,2-(ethylenedioxy)diethanethiol, 2.5 $_{vol}$% H_2O, 1 $_{vol}$% TIS. The crude peptide was purified by RP-HPLC on C18 semi-preparative column. Purity: 96%. Ret. Time: 32.56 min. The HPLC trace of crude product is reported in Figure 11. The HPLC trace and the MALDI-TOF spectra of the purified compound are shown in Figure 2.

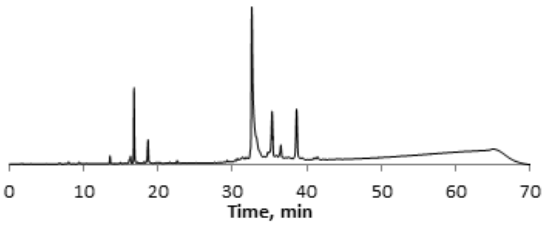

Figure 11: HPLC traces (detection wavelength: 220 nm) for crude product **1**.

Natural trp-zipper: Ac-Ser-Trp-Thr-Trp-Glu-Gly-Asn-Lys-Trp-Thr-Trp-Lys-NH_2

The peptide was synthesized on a 0.1 mmol scale by standard protocol of Fmoc chemistry SPPS. Sieber resin was used (0,65 mmol/g). Fmoc-Trp-OH, Fmoc-Lys(Trt)-OH, Fmoc-Thr(Trt)-OH, Fmoc-Glu(OtBu)-OH, Fmoc-Ser(Trt)-OH, Fmoc-Gly-OH, Fmoc- Asn(Trt)-OH were used. The coupling step was performed with 5 eq Fmoc-protected amino acid, 5 eq HBTU and 10 eq DIPEA (2 x 45 min). The Fmoc-deprotection step was performed with 20% piperidine in DMF (1 x 30 min). The product was obtain from the peptide synthesizer. The last Fmoc-deprotection step was performed with 20% piperidine in DMF (1 x 30 min). The acetylation step was performed with 10 eq Ac_2O, 0.1 eq HOBt and 10 eq DIPEA. Cleavage from the resin was performed at 0 °C for 1 h with 95% TFA, 2.5 $_{vol}$% tri-*iso*-propylsilane (TIS), 2.5 $_{vol}$% H_2O. The crude peptide was purified by RP-HPLC on C18 semi-preparative column. Purity: 98%. Ret. Time: 21.02 min.

a b

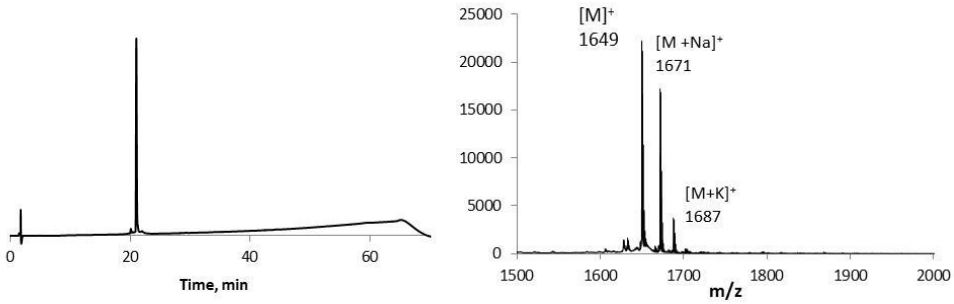

Figure 12: a) HPLC trace (detection wavelength: 220 nm) for purified product. b) MALDI-TOF spectrum for the product.

5.5.2 Spectroscopic studies

Isomerization cycle for compound 1: UV-vis and NMR spectroscopy and HPLC were used to follow the isomerization steps of compound **1**. The cycle is shown in Figure 1.
HPLC was used to determine the PSS (photostationary state) ratio's. A sample of compound *trans*-**1** (1 mg/mL) was prepared in 50:50 milliQ water:acetonitrile and analyzed by HPLC. The sample was irradiated for 2 min at λ = 312 nm, to obtain unstable *cis*-**1**, and analysed. Subsequently it was left for 4h at 60 °C, to obtain stable *cis*-**1**, followed by HPLC analysis. The HPLC traces are reported in Figure 4.
UV-vis spectroscopy was used to determine the activation parameters. The same procedure as reported for compound **3** was used. The temperature used are 40 °C, 45 °C, 50 °C, 55 °C and 60 °C. The data are reported in Figure 4.

Isomerization cycle for compound 3: UV-vis and NMR spectroscopy were used to follow the isomerization steps of compound **3**. The cycle is shown in Figure **13**.
NMR was used to determine the PSS ratio (photostationary state) and the UV-vis spectroscopy to determine the $t_{1/2}$ and the thermodynamic parameters.

For NMR studies, a solution of compound **3** (5 mg in 500 uL CD_3OD or DMSO-d_6) was irradiated with λ=312 nm until the photostationary state was reached. The PSS ratio stable *trans* - unstable *cis* isomerization is 14:86 in CD_3OD and 3:97 in DMSO. In CD_3OD, unstable *cis*-**3** precipitates from the solution. Afterwards the precipitate was filtered off and redissolved in CD_3OD to obtain a solution of unstable *cis*-**3** (3mg in 300 uL) was prepared and warmed up at 40 °C. Partial ^{1}H-NMR spectra are shown in Figure 3.

Unstable *cis*-3: ^{1}H NMR (400 MHz, CD_3OD) δ 7.94 (d, *J* = 8.2 Hz, 4H, arom), 7.35 (d, *J* = 8.3 Hz, 4H, arom), 6.88 (s, 2H, arom), 4.05(s, 4H, C**H**$_2$ Gly), 3.62 (m, 2H, C**H**CH_3), 2.70 (dd, *J* = 15.8 Hz, 7.8 Hz, 2H, C**H**$_2$$CHCH_3$), 2.29 (s, 6H, C**H$_3$** ar), 1.53 (d, *J* = 6.0 Hz, 6H, CHC**H$_3$**), 1.36 (s, 6H, C**H$_3$** ar).

Stable *cis*-3: ^{1}H NMR (400 MHz, CD_3OD) δ 8.00 (d, *J* = 8.4 Hz, 4H, arom), 7.41 (d, *J* = 8.4 Hz, 4H, arom), 6.91 (s, 2H, arom), 4.08 (s, 4H, C**H**$_2$ Gly), 3.14 (dd, *J* = 14.9 Hz, 5.9 Hz, 2H, C**H**$_2$CHCH$_3$), 2.57 (d, *J* = 15.0 Hz, 2H, C**H**$_2$CHCH$_3$), 2.29 (s, 6H, C**H**$_3$ ar), 1.45 (s, 6H, C**H**$_3$ ar), 1.14 (d, *J* = 6.8 Hz, 6H, CHC**H**$_3$).

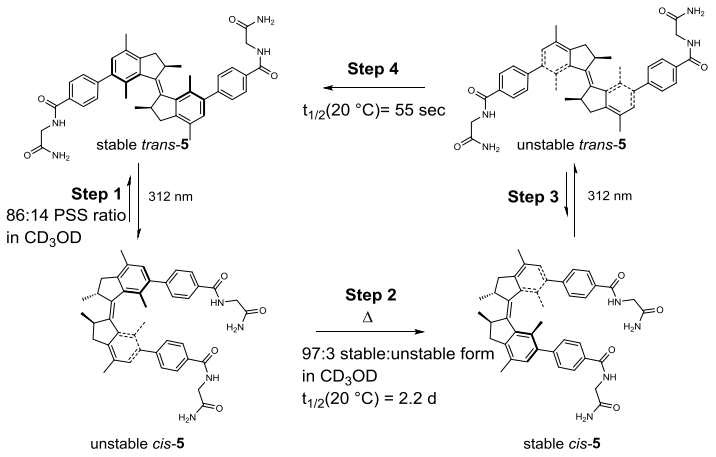

Figure 13: Isomerisation cycle for compound **3**, half-life values and PSS ratio's.

For UV-vis spectroscopy, a $1 \cdot 10^{-5}$ M solution of stable *trans*-**3** in MeOH was prepared and the spectrum of trans-**3** was recorded at 30 °C. The solution was irradiated at λ = 312 nm and the absorbance spectra were recorded till the photostationary state was reached (Figure 14). Next, a filter (cut-off λ = 340 nm) was positioned between the sample and the light source and the decrease in absorbance at λ = 350 nm was recorded. This permits, with a simple exponential decay curve, to calculate the rate constant, k. This procedure was repeated at 40 °C, 50 °C and 60 °C (Figure 4). Using the Eyring equation, the kinetic constants and the half-life time, $t_{1/2}$, of two thermal isomerization processes were calculated (Figure 4).
The same experiment was repeated for stable *cis*-**3** ($1 \cdot 10^{-5}$ M in MeOH) at 0 °C, -5 °C, -10 °C and -15 °C (Figure 15).

$$\frac{\ln k}{T} = -\frac{\Delta H^{\ddagger}}{R} \cdot \frac{1}{T} + \frac{\ln k_B}{h} + \frac{\Delta S^{\ddagger}}{\mathrm{R}}$$

where k is reaction rate constant, T is absolute temperature, $\Delta H^{\ddagger}$ is the enthalpy of activation, R is gas constant, k_B is Boltzmann constant, h is Plank's constant and $\Delta S^{\ddagger}$ is the entropy of activation.
Clear isosbestic points were found at λ = 318 nm for the isomerization from stable *trans* to unstable *cis* form and at λ = 330 nm for the isomerization from unstable *cis* to stable *cis* form.

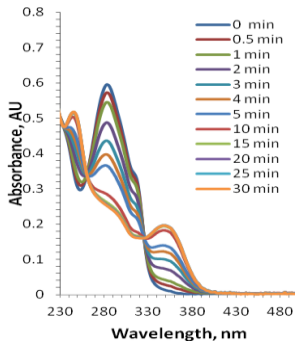

Figure 14: a) Changes in UV/vis spectrum upon irradiation at λ = 312 nm of compound *trans*-**3** ($1 \cdot 10^{-5}$ M in methanol).

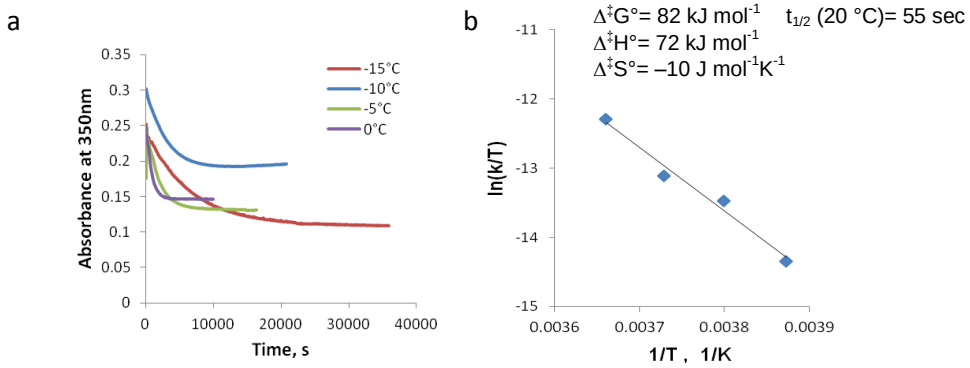

Figure 15: a) Exponential decrease of the absorption band at λ = 350 nm for unstable *trans*-**3** at different temperatures. b) Eyring plot for the thermal isomerization from unstable *trans*-**3** to stable *trans*-**3** and activation parameters.

CD Spectroscopy for compound 4: A 24 uM solution of stable *trans*-**4** in MeOH at 20 °C was irradiated at λ = 312 nm and then warmed at 40 °C. CD spectra were recorded before and after irradiation at λ = 312 nm and after warming. For each isomer, CD spectra were recorded at 5 °C and 20 °C. Spectra are shown in Figure 5. The UV-vis spectra are shown in Figure 16.

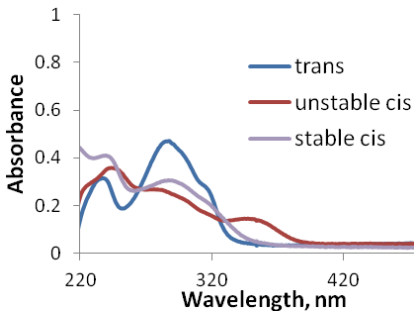

Figure 16: UV-Vis spectra of *trans*-**4** unstable *cis*-**4** and stable *cis*-**4**.

CD Spectroscopy for compound 1: A 24 uM solution of stable *trans*-**1** in MeOH at 20 °C was irradiated at λ = 312 nm and then warmed at 40 °C. CD spectra were recorded before and after irradiation at λ = 312 nm and after warming. For each isomer, CD spectra were recorded at different temperatures, between -10 °C and 40 °C. Spectra are shown in Figure 5 and UV-vis spectra are shown in Figure 17.

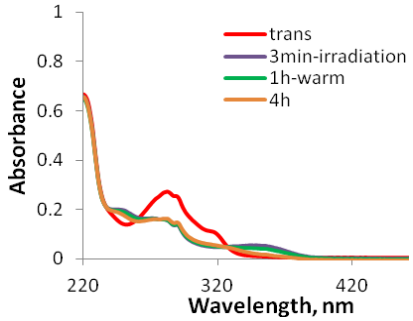

Figure 17: UV-Vis spectra of *trans*-**1**, unstable *cis*-**1** and stable *cis*-**1**.

Temperature dependency for CD signal at 228 nm for compound 1: A 24 uM solution of stable *trans*-**1** in MeOH was prepared. The solution was irradiated at λ = 312 nm and then warmed to 40 °C. CD spectra was recorded before and after irradiation at λ = 312 nm and after warming. For every isomer, CD spectra were recorded from 0 °C till 40 °C with intervals of 5 °C. Spectra are shown in Figure 18 and Figure 5.

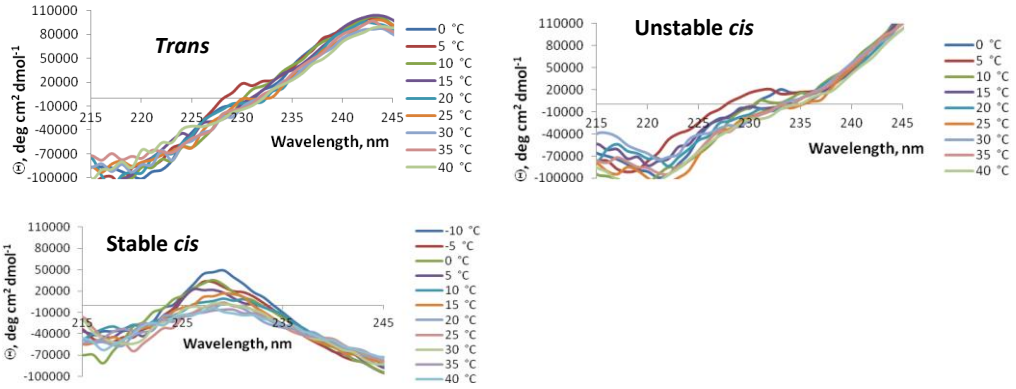

Figure 18: CD spectra (215-245 nm region) of *trans*-**1**, unstable *cis*-**1** and stable *cis*-**1** at different temperatures.

Temperature dependency for CD signal at 228 nm for natural trp-zipper: A 71 uM solution of **8** in MeOH was prepared. CD spectra were recorded from -10 °C till 40°C with interval of 5 °C. Spectra are shown in Figure 5 and the UV-vis spectra in Figure 19.

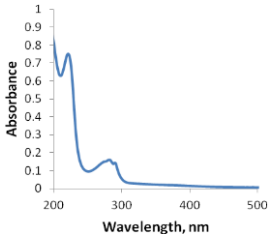

Figure 19: UV-vis spectrum of natural trp-zipper.

5.5.3 2D-NMR studies on compound 1

A solution of compound **1** (1.8 mg in 300 uL methanol-d3) was used. A set of COSY, TOCSY, NOESY were recorded for the three species. The unstable *cis* was obtained by irradiation at λ = 312 nm of the *trans*-**1** for 30 min and the stable *cis* was obtained by warming the sample of unstable *cis*-**1** to 50 °C for 5 h. The 1D-NMR spectra reported in Figure 20 and Figure 7 show the isomerization steps.

***Trans*-trp-zipper-overcrowded alkene**

AA	NH	Alpha-H	Others
Ac			
Ser-1	8.07	4.09	3.65, 3.57 β-H
Trp-2	7.87	4.57	3.20 β-H
Thr-3	7.54	3.97	3.96 β-H, 0.73 γ-H
Trp-4	7.61	4.57	
Glu-5	7.78	4.20	1.88, 2.04 β-H, 2.18 γ-H
Switch	8.40(Mot), 7,58 (Glu)		3.55, 3.50 Switch-NH-C**H**$_2$, 3.42 Glu-NH-C**H**$_2$ 6.86 arom singlet (Glu), 6.93 arom singlet (Lys) 7.79 (ortho), 7.47 (meta) Lys 7.91 (ortho), 7.43 (meta) Glu 2.22 arom CH_3 (Glu), 2.27 arom CH_3 (Lys) 1.07,1.11 CHC**H**$_3$ 3.02, C**H**CH_3 2.35, 2.72 C**H**$_2$CHCH_3
Lys-6	8.55	4.34	1.76, 1.57, 1.28 (δ), 2.80- 2.02(ε?)
Trp-7	7.99	4.70	
Thr-8	7.61	4.23	4.13 β-H, 0.94 γ-H
Trp-9	7.97	4.57	
Lys-10	7.87	4.22	1.77,1.53, 1.30 (δ), 2,85-2.07(ε?)
NH2			

Aromatic protons for Trp

A	B	C	D	E	F
7.60	7.03	7.10	7.32	7.20	10.34
7.56	7.97	7.06	7.30	7.12	10.37
7.54	6.95	7.03	7.29	7.12	10.28
7.49	6.96	7.06	7.3	7.18	10.27

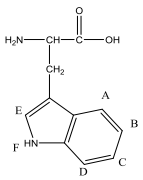

NOE interactions

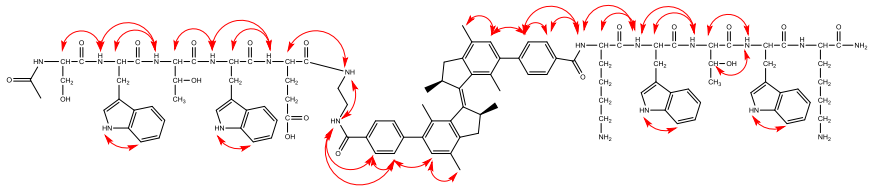

Stable *cis*-trp-zipper-overcrowded alkene

AA	NH	Alpha-H	Others
Ac			2.18
Ser-1	8.11	4.07	3.68, 3.59 β-H
Trp-2			β-H
Thr-3	7.59	3.92	3.89 β-H, 0.69 γ-H
Trp-4			
Glu-5	8.06	4.20	2.20 β-H γ-H
Switch	8.41 (Mot), 7.75 (Glu)		3.38 SwitchNH-C**H**$_2$, 3.65 Glu-NH-C**H**$_2$ 6.85 arom singlet (Glu), 6.77 arom singlet (Lys) 7.36 (ortho), 7.92 (meta) Lys 7.37 (ortho), 7.95 (meta) Glu 2.26 arom CH_3 (Glu) external, 1.45 internal 2.24 arom CH_3 (Lys) external, 1.37 internal 1.13 CHC**H**$_3$ 3.45 C**H**CH_3 2.56, 3.12 C**H**$_2$$CHCH_3$
Lys-6	8.68	4.26	1.67, 1.56 (δ or γ or β), 2.77 (ε)
Trp-7	8.13	4.73	3.28, 3.16
Thr-8	7.77	4.22	4.09 β-H, 0.92 γ-H
Trp-9	8.06	4.56	3.19
Lys-10	7.90	4.23	1.27, 1.55, 1.78 (δ or γ or β),3.21 (ε)
NH2			

Trp:

NH	Alpha-H	Others
7.95	4.54	3.15
7.61	4.53	3.08, 3.15 β-H

Aromatic protons for Trp :

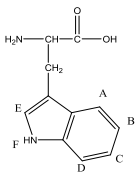

A	B	C	D	E	F
7.45	6.87	6.93	7.19	6.94	10.14
7.53	6.99	7.07	7.30	7.14	10.29
7.21 7.42	6.95 6.88	6.80 7.02	6.88 7.27	7.08 7.07	10.34 10.09

In yellow: The A, B, C, D system has not been correlated with E, F system.

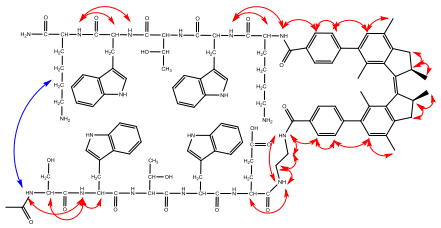

Stable *cis*-trp-zipper-overcrowded alkene (5 °C)

AA	NH	Alpha-H	Others
Ac			2.18
Ser-1	8.26	4.09	3.68, 3.58 β-H
Trp-2	8.11	4.55	3.28, 3.15 β-H
Thr-3	7.68		3.89 β-H, 0.66 γ-H
Trp-4	7.68		
Glu-5	7.8	4.13	1.89, 2.03 β-H, 2.14 γ-H
Switch	8.50 (Mot), 7.80 (Glu)		3.36 SwitchNH-C**H**$_2$, 3.64 Glu-NH-C**H**$_2$ 6.86 Arom singlet (Glu), 6.80 Arom singlet (Lys) 7.37 (ortho), 7.94 (meta) Lys 7.38 (ortho), 7.96 (meta) Glu 2.26 arom CH_3 (Glu) external, 1.43 internal 2.24 arom CH_3 (Lys) external, 1.36 internal 1.08, 1.13 CHC**H**$_3$ 3.46 C**H**CH_3 2.55, 3.12 C**H**$_2$$CHCH_3$
Lys-6	8.74	4.20	1.63, 1.53 (δ or γ or β)
Trp-7	8.22	4.75	3.29, 3.14
Thr-8	7.68	4.14	4.09 β-H, 0.93 γ-H
Trp-9	8.19	4.56	3.26, 3.18
Lys-10	8.04	4.23	1.24, 1.52, 1.80 (δ or γ or β)
NH2			

Aromatic protons for Trp :

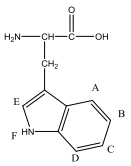

Trp	A	B	C	D	E	F
2	7.40	7.00	6.85	7.26	7.10	10.44
4	7.29	6.95	6.79	7.20	6.94	10.25
7	7.46	6.94	6.86	7.19	7.06	10.18
9	7.51	7.06	6.99	7.30	7.14	10.38

In same colors: Protons that have a correlation in NOESY.

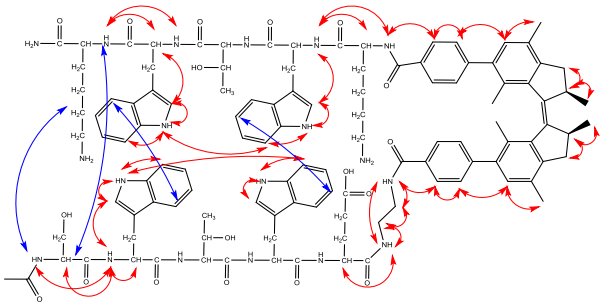

Irradiation at 312 nm

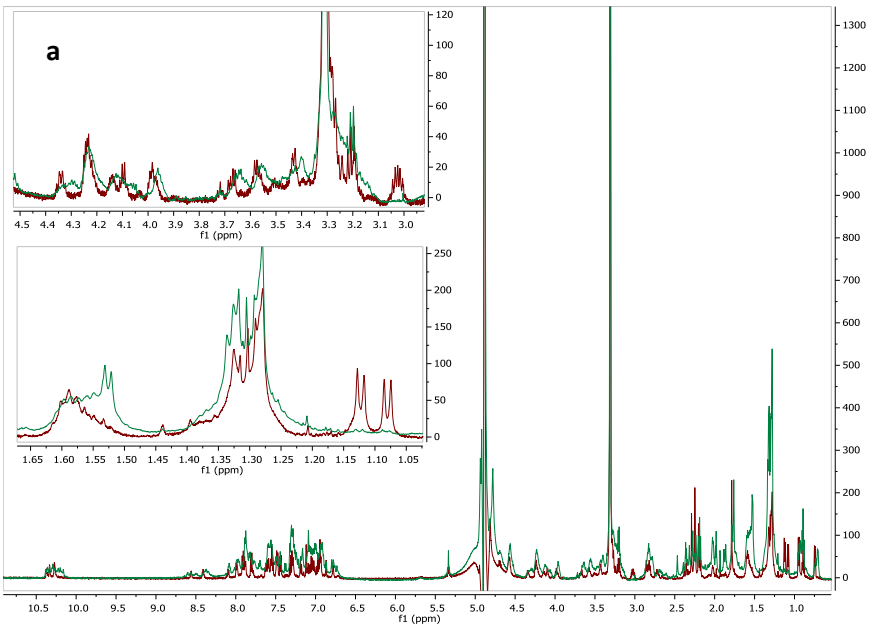

Warming up

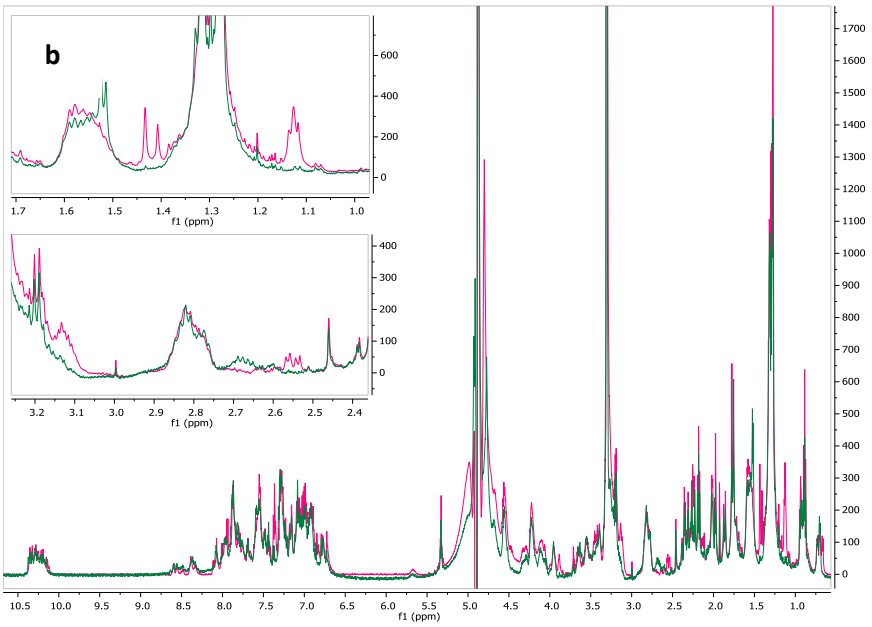

Figure 20: ^{1}H-NMR spectra of various isomers in rotary cycle of compound **1** (1.8 mg in 300 uL methanol-d3). a) NMR spectra before (red line) and after (green line) irradiation at λ= 312 nm for 30 min. b) NMR spectra before (green line) and after (pink line) warming up at 60 °C for 4 h. The expanded regions (inset) correspond to the CH_3 in the connected to the aromatic system.

5.5.3 Transmission Electron Microscopy

TEM measurements for compound 1

Preparation of TEM-samples. Samples for transmission electron microscopy were placed on carbon-coated 400 mesh copper grids. After 1 min of adhesion, the sample was removed by filter paper and stained with 2% uranyl acetate and dried with filter paper. The samples were measured in a Philips CM120 or FEI T20 electron microscope operating at 120 or 200 keV.

Solutions of compound *trans*-**1** and stable *cis*-**1** (1.8 mg in 300 uL methanol-d3) were analysed. The images are shown in Figure 8.

Cryo-TEM measurements for compound 1

Preparation of cryo TEM-samples. 3 µl sample was placed on a glow discharged holy carbon coated grid (Quantifoil 3.5/1) and blotted. Samples were subsequently vitrified in liquid ethane (FEI, Vitrobot). The samples were observed in a Philips CM120 or FEI T20 electron microscope operating at 120 or 200 keV using a Gatan cryo-stage. Images were recorded under low-dose conditions using a slow-scan CCD camera.

First procedure: A solution of *trans*-**1** in milliQ water (1 mg/mL) was prepared. The sample was irradiated for 5 min at λ = 312 nm to form unstable cis and then warmed up to 45 °C for 5 h. Cryo TEM images were taken before and after irradiation and after warming. Before taking the TEM images, a UV-vis sample was prepared to examine the composition of the system: 2 uL of the aqueous solution were taken and diluted with 200 uL of a different solvent (acetonitrile or methanol) (Figure 21). The images are shown in Figure 9.

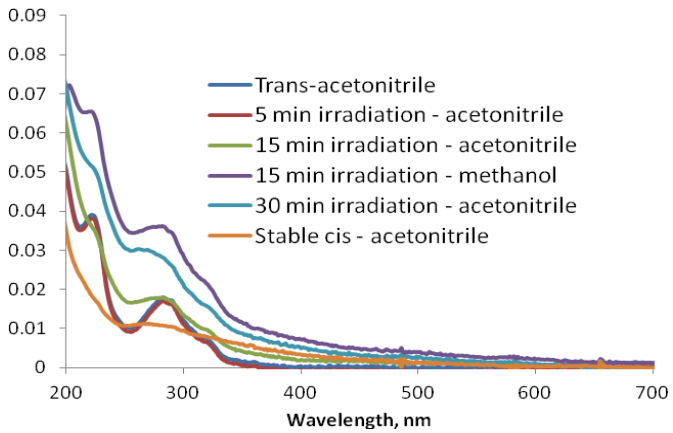

Figure 21: UV-vis spectra of *trans*-**1** at indicated stages during the irradiation process.

Second procedure: A second sample was prepared in MeOH (0.1 mg in 2 mL), irradiated for 5 min at λ= 312 nm to form unstable *cis*-**1**, the solvent was evaporated and 50 uL of milliQ water were added. 1 mL was then warmed up to 45 °C for 5 h, the solvent was evaporated and 50 uL of milliQ water was added (Figure 22).

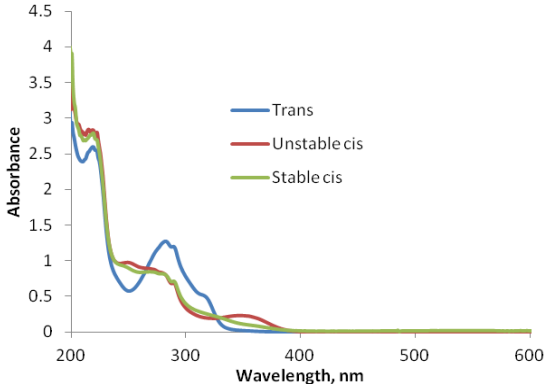

Figure 22: UV-vis spectra of *trans*-**1,** *unstable cis*-**1,** *stable cis*-**1** in methanol.

Unstable *Cis* (Second Procedure)

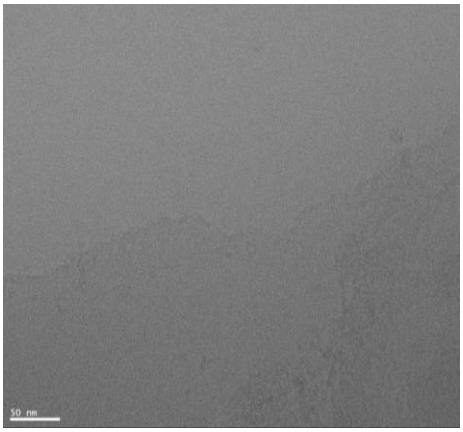

Stable *Cis* (Second Procedure)

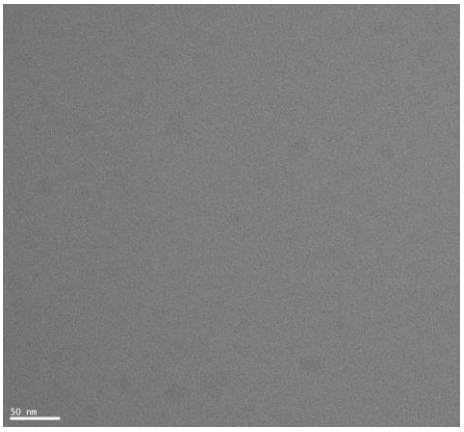

5.6 References

[1] P. Westermark, M. D. Benson, J. N. Buxbaum, A. S. Cohen, B. Frangione, B. S.-I. Ikeda, C. L. Masters, G. Merlini, M. J. Saraiva, J. D. Sipe, *Amyloid,* 2007, **14**, 179.

[2] T. M. Doran, E. A. Anderson, S. E. Latchney, L. A. Opanashuk, B. L. Nilsson, *J. Mol. Biol.* 2012, **421**, 315.

[3] E. D. Roberson, L. Mucke, *Science*, 2006, **314**, 781.

[4] G. Hopping, J. Kellock, B. Caughey, V. Daggett, *ACS Med. Chem. Lett*. 2013, **4**, 824.

[5] K. Rajagopal, M. S. Lamm, L.-A. Haines-Butterick, D. J. Pochan, J. P. Schneider, *Biomacromolecules* 2009, **10**, 2619.

[6] D. J. Pochan, J. P. Schneider, J. Kretsinger, B. Ozbas, K. Rajagopal, L. Haines, *J. Am. Chem. Soc.* 2003, **125**, 11802.

[7] B. Ozbas, J. Kretsinger, K. Rajagopal, J. P. Schneider, D. J. Pochan, *Macromolecules* 2004, **37**, 7331.

[8] W. Szymański, J. M. Beierle, H. A. V. Kistemaker, W. A. Velema, B. L. Feringa, *Chem. Rev.* 2013, **113**, 6114.

[9] A. A. Beharry, G. A. Woolley, *Chem. Soc. Rev.,* 2011, **40**, 4422.

[10] T. M. Doran, D. M. Ryan, B. L. Nilsson, *Polym. Chem.* 2014, **5**, 241.

[11] T. M. Doran, E. A. Anderson, S. E. Latchney, L. A. Opanashuk, B. L. Nilsson, *ACS Chem. Neurosci.* 2012, **3**, 211.

[12] A. Aemissegger, V. Kräutler, W. F. van Gunsteren, D. Hilvert, *J. Am. Chem. Soc.* 2005, **127**, 2929.

[13] S.-L. Dong, M. Löweneck, T. E. Schrader, W. J. Schreier, W. Zinth, L. Moroder, C. Renner, *Chem. Eur. J.* 2006, *12*, 1114.

[14] M. Erdélyi, A. Karlén, A. Gogoll, *Chem. Eur. J*. 2005, **12**, 403.

[15] N. Regner, T. T. Herzog, K. Haiser, C. Hoppmann, M. Beyermann, J. Sauermann, M. Engelhard, T. Cordes, K. Ruck-Braun, W. Zinth, *J. Phys. Chem. B* 2012, **116**, 4181.

[16] A. A. Deeg, T. E. Schrader, S. Kempter, J. Pfizer, L. Moroder, W. Zinth, *ChemPhysChem* 2011, **12**, 559.

[17] C. Hoppmann, C. Barucker, D. Lorenz, G. Multhaup, M. Beyermann, *Chembiochem* 2012, **13**, 2657.

Hoppmann, C.; Barucker, C.; Lorenz, D.; Multhaup, G.; Beyermann, M. *Chembiochem* **2012**, *13*, 2657.

[18] J. Wang, B. L. Feringa, *Science,* 2011, **18**, 1429.

[19] M. Vlatković, L. Bernardi, E. Otten, B. L. Feringa, *Chem. Commun*. 2014, **50**, 7773.

[20] J. Wang, J.; L. Hou, W. R. Browne, B. L. Feringa, *J. Am. Chem. Soc.,* 2011, **133**, 8162.

[21] S. J. Wezenberg, M. Vlatković, J. C. M. Kistemaker, B. L. Feringa, *J. Am. Chem. Soc.,* 2014, **136**, 16784.

[22] a) A. G. Cochran, N. J. Skelton, M. A. Starovasnik, *Proc. Natl. Acad. Sci. USA,* 2001, **98**, 5578. b) A. G. Cochran, N. J. Skelton, M. A. Starovasnik, *Proc. Natl. Acad. Sci. USA,* 2002, **99**, 9081.

[23] A. A. Deeg, M. S. Rampp, A. Popp, B. M. Pilles, T. E. Schrader, L. Moroder, K. Hauser, W. Zinth, *Chem. Eur. J*., 2014, **20**, 694.

[24] N. Koumura, R. W. J. Zijlstra, R. A. van Delden, N. Harada, B. L. Feringa, *Nature,* 1999, **401**, 152.

[25] J. Chen, J. C. M. Kistemaker, J. Robertus, B. L. Feringa, *J. Am. Chem. Soc.* 2014, **136**, 14924.

[26] I. B. Grishina, R. W. Woody, *Faraday Discuss*., 1994, **99**, 245.

[27] K. Wüthrich, NMR of Proteins and Nucleic acids, Wiley, New York, 1986.

[28] J. R. Lewandowski, P. C. A. van der Wel, M. Rigney, N. Grigorieff, R. G. Griffin, *J. Am. Chem. Soc.* 2011, **133**, 14686.

[29] W. S. Childers, N. R. Anthony, A. K. Mehta, K. M. Berland, D. G. Lynn, *Langmuir,* 2012, **28**, 6386.

[30] D. Galante, A. Corsaro, T. Florio, S. Vella, A. Pagano, F. Sbrana, M. Vassalli, A. Perico, C D'Arrigo, *Int. J. Biochem. Cell B.* 2012, **44**, 2085.

[31] N. Norlin, M. Hellberg, A. Filippov, A. A. Sousa, G. Gröbner, R. D. Leapman, N. Almqvist, O. N. Antzutkin, *J. Struct. Biol.,* 2012, **180**, 174.

[32] Alzheimer's Disease, Cellular and Molecular Aspects of Amyloid β, Ed. Robin Harris J., Fahrenholz F., *Subcellular Biochemistry* 2005, vol. 38, p. 1.

[33] S. Gilead, E. Gazit, *Supramol. chem.,* 2005, **17**, 87.

[34] M. C. A. Stuart, J. C. van de Pas, J. B. F. N. Engberts, *J. Phys. Org. Chem*. 2005, **18**, 929.